JACS
JOURNAL OF THE AMERICAN CHEMICAL SOCIETY
Communication
pubs.acs.org/JACS

Redox Non-Innocence of a *N*-Heterocyclic Nitrenium Cation Bound to a Nickel–Cyclam Core

Florian Heims,[§] Florian Felix Pfaff,[§] Sarah-Luise Abram,[§] Erik R. Farquhar,[‡] Maurizio Bruschi,[#] Claudio Greco,[#] and Kallol Ray*[,§]

[§]Institut für Chemie, Humboldt-Universität zu Berlin, Brook-Taylor-Straße 2, D-12489 Berlin, Germany

[‡]Case Western Reserve University Center for Synchrotron Biosciences and Center for Proteomics and Bioinformatics, National Synchrotron Light Source, Brookhaven National Laboratory, Upton, New York 11973, United States

[#]Department of Earth and Environmental Sciences, University of Milano-Bicocca, Piazza della Scienza 1, 20126 Milan, Italy

Supporting Information

ABSTRACT: The redox properties of Ni complexes bound to a new ligand, $[DMC\text{-}nit]^+$, where a *N*-heterocyclic nitrenium group is anchored on a 1,4,8,11-tetraazacyclotetradecane backbone, have been examined using spectroscopic and DFT methods. Ligand-based $[(DMC\text{-}nit)Ni]^{2+/+}$ reduction and metal-based $[(DMC\text{-}nit)Ni]^{2+/3+}$ oxidation processes have been established for the $[(DMC\text{-}nit)Ni]^{+/2+/3+}$ redox series, which represents the first examples of nitrenium nitrogen (N_{nit})-bound first-row transition-metal complexes. An unprecedented bent binding mode of N_{nit} in $[(DMC\text{-}nit)Ni]^{2+}$ is observed, which possibly results from the absence of any $N_{nit}\rightarrow Ni$ σ-donation. For the corresponding $[(DMC\text{-}nit)Ni(F)]^{2+}$ complex, σ-donation is dominant, and hence a coplanar arrangement at N_{nit} is predicted by DFT. The binding of the triazolium ion to Ni enables new chemistry (formate oxidation) that is not observed in a derivative that lacks this functional group. Thus the *N*-heterocyclic nitrenium ligand is a potentially useful and versatile reagent in transition-metal-based catalysis.

Transition-metal complexes are at the heart of organometallic chemistry and homogeneous catalysis.[1] Very often the bound ligands are anionic or neutral species. However, cationic ligands ligated to a transition metal are also known in a few cases.[2,3] Notably, for the positively charged ligands (L^+), π-acidity rather than σ-basicity of L^+ must be considered as the decisive factor for the stability of their transition-metal complexes, and the efficacy of stabilizing influences such as low formal oxidation state and high atomic number of the metal (M) can be traced to the stabilization of the $M\rightarrow L^+$ π-bond. The weaker π-acceptance ability of a cationic N atom, relative to P and As atoms, may explain why the nitrenium ion has the weakest binding ability among all the *N*-heterocyclic carbene-type ligands of the Group 15 p-block elements.[3] Notably, *N*-heterocyclic nitrenium (NHN) ions were, until very recently, unknown to behave as ligands. By incorporating the triazolium ring within a pincer-type system, Gandelman et al.[3a] demonstrated coordination of nitrenium ions to electron-rich transition metals like Rh(I) and Ru(II) in both the solid and solution states. This study filled a missing link in the series of both fundamentally and practically important *N*-heterocyclic carbenes and their analogues, which have become ubiquitous in the fields of transition metal and organic catalysis.[4]

Interestingly, all reported [(NHN)-M] (M = Ru(II), Rh(I)) complexes are found to be planar at the nitrenium nitrogen (N_{nit}) atom.[3a] However, in the complexes of the *N*-heterocyclic phosphenium and arsenium ligands, which are heavier analogues of NHN, both planar and pyramidal geometries at the central P or As atoms have been observed.[3] Whereas both σ-donation from the filled sp^2 hybrid orbital of P or As and π-acceptance into the unoccupied p-π orbital ensure planar coordination, the presence of a π-interaction alone results in a pyramidal geometry at P or As.[3e] We initiated the present study to investigate whether the planar geometric situation would persist for NHN complexes of first-row transition metals, which are weaker σ-donors and π-acceptors, as compared to their heavier congeners. Accordingly, we designed a new ligand system $[DMC\text{-}nit]^+$, where a triazolium ring is anchored on a well-investigated[5,6] cyclam (1,4,8,11-tetraazacyclotetradecane) backbone, and studied its coordination chemistry with nickel.

Coupling of the nitrenium precursor 1,3-di-(2′-bromoethyl)-benzotriazolium bromide[3a] with 1,8-dimethyl-1,4,8,11-tetraazacyclotetradecane in a basic medium led to initial formation of the benzotriazolium-capped cyclam bromide (Figures S1 and S2), which upon anion exchange with KPF_6 or $NaBPh_4$ yielded the desired $[DMC\text{-}nit]^+$ ligand cation (Scheme S1) as PF_6^- or BPh_4^- salts (Figures S3–S5). Reactions of equimolar amounts of [DMC-nit]X (X = PF_6 or BPh_4) and $Ni(cod)_2$ (cod = 1,5-cyclooctadiene) in CH_3CN afforded the purple $[(DMC\text{-}nit)Ni]X_2$ ($[\mathbf{1}]\text{-}(X)_2$; X = PF_6 or BPh_4) complexes in ~35–50% yield (Scheme 1); formation of $[\mathbf{1}]\text{-}(X)_2$ is accompanied by $1e^-$ oxidation of Ni(0) and concomitant reduction of [DMC-nit]X, in agreement with the observation that the yields of $[\mathbf{1}]\text{-}(X)_2$ never exceeded 50% of the ligand. Electrospray ionization mass spectrometry (ESI-MS) of $[\mathbf{1}]\text{-}(PF_6)_2$ shows a prominent peak at m/z = 458.259 (calcd: 458.254) (Figure S6). X-ray analysis of single crystals of $[\mathbf{1}]\text{-}(PF_6)_2$ confirmed coordination of $[DMC\text{-}nit]^+$ as a pentadentate ligand, with the cyclam macrocycle adopting a *trans-I* configuration[6] and the central nitrogen (N_{nit}) of the benzotriazolium residue bound at the

Received: October 2, 2013
Published: December 20, 2013

dx.doi.org/10.1021/ja4099559 | J. Am. Chem. Soc. 2014, 136, 582–585

Scheme 1. Formation of $[1]^{2+}$, $[2\text{-F}]^{2+}$, and $[3]^{+}$ and the Reactivity of $[2\text{-F}]^{2+}$ with Formate[a]

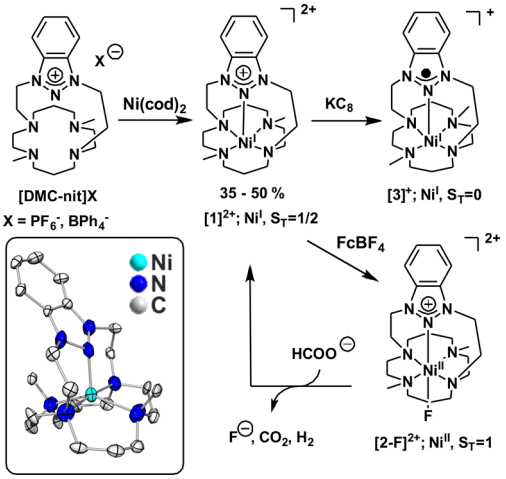

[a]The central nitrogen of the benzotriazolium residue is called N_{nit} herein. Inset: Structure of one of the two crystallographically independent molecules in crystals of $[1]\text{-}(PF_6)_2$. S_T = total spin.

apical position of a distorted square pyramid (SQP; $\tau = 0.48$;[7] Scheme 1 inset). Interestingly, $[1]\text{-}(PF_6)_2$ is pyramidal at the N_{nit} center and has a coordination geometry (sum of all angles ($\angle_{sum}$) = 332°)[7] consistent with a nonbonding lone pair still present on N_{nit}. Thus, in contrast to the previously reported benzotriazolium-bound Rh(I) complexes,[3a] which involved both σ- and π-interactions leading to a coplanar arrangement, the bonding in $[1]\text{-}(PF_6)_2$ can be described as primarily M→L^+ π-bonding; the lone pair of electrons on N_{nit}, located in the sp^2 hybrid orbital, do not participate in bonding to the metal center (see also results of DFT calculation below).

Cyclic voltammetry (CV) of $[1]\text{-}(X)_2$ (X = PF_6 or BPh_4) in CH_3CN at room temperature reveals one reversible oxidation wave centered at −0.51 V vs Fc^+/Fc and a reversible reduction wave centered at −1.71 V (Figures 1 and S7) in each case.

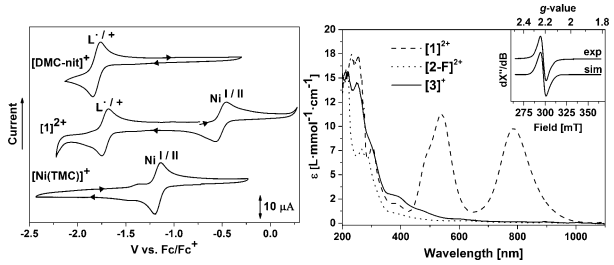

Figure 1. Left: Cyclic voltammetry of $[DMC\text{-}nit]^+$, $[1]\text{-}(PF_6)_2$, and [(TMC)Ni]OTf complexes recorded in CH_3CN solutions containing 0.10 M NBu_4PF_6. $L^{\bullet/+}$ represents the $[(DMC\text{-}nit)]^{+/0}$ couple. Right: Absorption spectra of $[1]^{2+}$, $[2\text{-F}]^{2+}$, and $[3]^+$ in CH_3CN at 25 °C. Inset: X-band EPR spectra of $[1]\text{-}(PF_6)_2$ in a frozen CH_3CN solution at 77 K. For simulation parameters see text and Figure S15.

Coulometric measurements show that both oxidation and reduction correspond to $1e^-$ processes. Interestingly, the CV of $[DMC\text{-}nit]^+$ exhibits a reversible reduction (−1.77 V vs Fc^+/Fc) at a potential very similar to the potential associated with the $[1]^{2+/+}$ process. The CV of the previously reported [(TMC)-Ni]OTf (TMC = 1,4,8,11-tetramethyl-1,4,8,11-tetraazacyclotetradecane) complex[8] was also measured for comparison, as it lacks the benzotriazolium residue. In this case a single reversible $Ni^{I/II}$ oxidation wave centered at −1.22 V vs Fc^+/Fc was observed. We assign the reduction in $[1]\text{-}(X)_2$ as ligand-centered and the oxidation as metal-centered, corroborated by X-ray absorption spectroscopy (XAS, see below). The 700 mV positive shift of the $Ni^{I/II}$ potential in $[1]\text{-}(X)_2$ relative to [(TMC)Ni]-OTf reflects the strong π-acceptance property of the bound benzotriazolium residue in $[1]\text{-}(X)_2$.

The absorption spectrum (Figure 1) of $[1]\text{-}(PF_6)_2$ displays two intense absorption maxima at 538 nm (ε = 11 500 M^{-1} cm^{-1}) and 786 nm (ε = 10 000 M^{-1} cm^{-1}). We tentatively assign these bands to metal-to-ligand charge-transfer type (Ni(I) to benzotriazolium transition), which are absent in [(TMC)Ni]-OTf,[8] as well as in the electrochemically generated $1e^-$-oxidized $[2]^{3+}$ and $1e^-$-reduced $[3]^+$ complexes. The EPR spectrum of a frozen solution of $[1]\text{-}(PF_6)_2$ (Figure 1) in CH_3CN at 77 K shows a slightly anisotropic signal (g_x = 2.22, g_y = 2.20, g_z = 2.18),[9] which supports the Ni(I) formulation of $[1]\text{-}(PF_6)_2$.

$[1]\text{-}(PF_6)_2$ can also be chemically oxidized by using 1 equiv of ferrocenium tetrafluoroborate in CH_3CN under anaerobic conditions to yield a green powder of $[(DMC\text{-}nit)Ni(F)](PF_6)_2$, $[2\text{-F}]\text{-}(PF_6)_2$, in ∼73% yield. $[2\text{-F}]\text{-}(PF_6)_2$ is EPR silent, and in its ^1H NMR spectrum (Figure S8) 12 paramagnetically shifted resonances are observed, which may indicate the presence of an octahedral (O_h) Ni(II) (d^8, S = 1) center (see XAS studies below). Interestingly, the number and relative integration of these resonances suggest that the *trans-I* configuration of the cyclam macrocycle is preserved in $[2\text{-F}]\text{-}(PF_6)_2$. ESI-MS (Figure S9) of a solution of isolated $[2\text{-F}]\text{-}(PF_6)_2$ in CH_3CN shows a prominent peak at m/z = 238.626 (calcd: 238.627), with an isotope distribution pattern consistent with its formulation as $[(DMC\text{-}nit)Ni(F)]^{2+}$. Subsequent studies showed that the presence of fluoride, possibly abstracted from the tetrafluoroborate anion, is necessary to stabilize the high positive charge of the $[(DMC\text{-}nit)Ni^{II}]^{3+}$ core in $[2\text{-F}]\text{-}(PF_6)_2$. Accordingly, $[2\text{-}CH_3CN]\text{-}(BPh_4)_3$ (O_h Ni^{II}; S = 1 from ^1H NMR; Figure S10), generated in the reaction of $[1]\text{-}(BPh_4)_2$ with ferrocenium tetraphenylborate, is extremely unstable. In the absence of any external fluoride donors and excess oxidant, it is spontaneously converted to the starting Ni(I) complex, $[1]\text{-}(BPh_4)_2$ (Figure S11); the electron necessary for the reduction of $[2\text{-}CH_3CN]\text{-}(BPh_4)_3$ to $[1]\text{-}(BPh_4)_2$ is presumably provided by the BPh_4^- anion.[10] EPR-silent yellowish-brown solutions of $[(DMC\text{-}nit)Ni]PF_6$ ($[3]\text{-}(PF_6)$) could be chemically generated by the reduction of $[1]\text{-}(PF_6)_2$ with excess KC_8. ^1H NMR of $[3]\text{-}(PF_6)$ shows all the resonances within δ = 0 to +10 ppm, confirming an S = 0 ground state; ESI-MS shows the molecular ion peak at m/z = 458.254 (Figure S12).

X-ray absorption near-edge spectroscopic studies (XANES; Figures 2A and S13) were performed at the Ni K-edge to directly probe the metal oxidation states in $[1]\text{-}(PF_6)_2$, $[2\text{-F}]\text{-}(PF_6)_2$, and $[3]\text{-}(PF_6)$ and provide support for the electrochemically derived assignments. $[1]\text{-}(PF_6)_2$ exhibits an edge inflection energy of ∼8341.2 eV, with a shoulder along the rising edge at 8336.3 eV corresponding to a 1s→4p shakedown transition,[11] in accord with the known SQP structure of this complex. A broad 1s→3d pre-edge peak is present at 8331.4 eV, with a peak area of ∼8.1 units. XANES of $[2\text{-F}]\text{-}(PF_6)_2$ shows a +2.8 eV blue-shift of the edge inflection energy to 8344.0 eV, relative to $[1]\text{-}(PF_6)_2$, supporting metal-centered oxidation to the Ni(II) state. The 1s→3d pre-edge transition has also blue-shifted by ∼0.5 to 8332.0 eV and weakened in intensity. Most notably, $[2\text{-F}]\text{-}(PF_6)_2$ lacks the diagnostic 1s→4p shakedown transition shoulder on the rising edge, providing strong evidence for a 6C O_h nickel site

dx.doi.org/10.1021/ja4099559 | J. Am. Chem. Soc. 2014, 136, 582−585

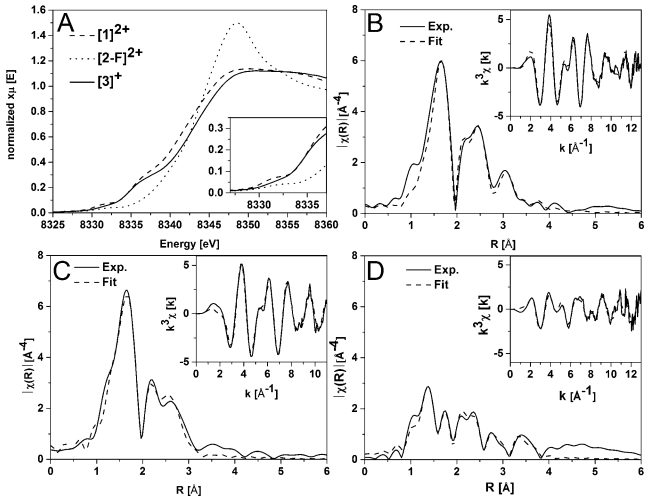

Figure 2. Normalized Ni K-edge XANES spectra for $[\mathbf{1}]$-$(PF_6)_2$, $[\mathbf{2}\text{-F}]$-$(PF_6)_2$, and $[\mathbf{3}]$-PF_6 (A) and the Fourier-transformed Ni K-edge EXAFS spectra of $[\mathbf{1}]$-$(PF_6)_2$ (B), $[\mathbf{2}\text{-F}]$-$(PF_6)_2$ (C), and $[\mathbf{3}]$-(PF_6) (D). Expansions of the 1s→3d and 1s→4p transitions are shown in the inset of (A). The insets of (B), (C), and (D) depict the $k^3\chi(k)$ EXAFS data and best fits.

in this complex.[11] Finally, XANES of $[\mathbf{3}]$-(PF_6) shows an unexpected 1.8 eV *blue-shift* in edge inflection energy to 8343.0 eV relative to $[\mathbf{1}]$-$(PF_6)_2$. This suggests that the reducing agent imparts a significant increase in the Ni effective nuclear charge (Z_{eff}). Most importantly, the existence of a 1s→3d pre-edge transition at an identical position (8331.4 eV) relative to $[\mathbf{1}]$-$(PF_6)_2$ indicates that $[\mathbf{3}]$-(PF_6) *does not* contain a d^{10} Ni^0 center. The Ni site in $[\mathbf{3}]$-(PF_6) is likely to still be 5C SQP, given that the 1s→4p shakedown transition is present at 8335.9 eV and similar in intensity to $[\mathbf{1}]$-$(PF_6)_2$.

Extended X-ray absorption fine structure (EXAFS) analysis reveals further structural details (Figure 2B–D). For $[\mathbf{1}]$-$(PF_6)_2$, the first coordination sphere could be satisfactorily fitted by five nitrogen scatterers at a distance of 2.11 Å (Table S1, fit 8). While the outer-shell features could be accounted for by several single scattering paths involving 14N/C at 2.94 Å, 4C at 3.45 Å, 2C at 3.97 Å, and 2C at 5.34 Å, the fit could be significantly improved by introducing multiple scattering paths involving elements of the cyclam and triazolium moieties. In general, the metrical parameters obtained for $[\mathbf{1}]$-$(PF_6)_2$ are in agreement with the molecular structure determined by X-ray crystallography, confirming that the solid-state structure is retained in frozen CH_3CN solutions of $[\mathbf{1}]$-$(PF_6)_2$. For $[\mathbf{2}\text{-F}]$-$(PF_6)_2$, the best fit (Table S1, fit 8) of the Ni EXAFS consists of two subshells of one fluorine scatterer at 1.93 Å and five nitrogen scatterers at 2.12 Å, supporting a six-coordinate Ni center in $[\mathbf{2}\text{-F}]$-$(PF_6)_2$, in agreement with the XANES and DFT studies (see below). Fits to a single shell of six nitrogen scatterers at 2.11 Å produced a significant decrease in fit quality (Table S1, fits 3 and 9). Analysis of the EXAFS data of $[\mathbf{3}]$-(PF_6) was less straightforward. $[\mathbf{3}]$-(PF_6) has much weaker EXAFS and Fourier-transform intensity compared to the other two complexes. The best fit (Table S1, fit 10) requires two subshells consisting of one nitrogen scatterer at 1.85 Å and three nitrogen scatterers at 2.06 Å. Notably, the latter shell has a very large Debye–Waller factor, consistent with a disordered distribution of bond lengths rather than a narrowly constrained range. We note that EXAFS supports a four-coordinate Ni center in $[\mathbf{3}]$-(PF_6), and the XANES points to a five-coordinate Ni site. DFT calculations for $[\mathbf{3}]$-(PF_6) (see below) show that both four- and five-coordinate states are feasible. Thus, the weak EXAFS intensity of $[\mathbf{3}]$-(PF_6) and large bond disorder may be attributable to destructive interference caused by the simultaneous existence of four- and five-coordinate Ni sites in the EXAFS sample of $[\mathbf{3}]$-(PF_6).

DFT calculations were carried out for the $[\mathbf{1}]^{2+}$, $[\mathbf{2}\text{-F}]^{2+}$, and $[\mathbf{3}]^{+}$ cations to obtain deeper insights into their electronic structures. For spin-doublet $[\mathbf{1}]^{2+}$, the computed Ni–N_{nit} distance, 2.082 Å, and average Ni–N(cyclam) distance, 2.18 Å, are in good agreement with the experimentally determined values of 2.021(3) and 2.149(3) Å, respectively (Table S2, Figure S14).[7] Moreover, the distorted SQP (τ = 0.48) geometry at Ni and the pyramidal geometry ($\angle_{sum}$ = 332°) at N_{nit} are well reproduced in the calculation (calcd: τ = 0.48 and $\angle_{sum}$ = 338).[7] Furthermore, the computational prediction of the EPR spectrum of $[\mathbf{1}]^{2+}$ is in good accord with the experiment (Table S3, Figure S15). Interestingly, the bent binding mode of N_{nit} is predicted to persist in the DFT-optimized structure of the hypothetical $[Ni^{I}(cyclam)(benzotriazolium)]^{2+}$ complex, which lacks any ethylene linkers between the cyclam and the benzotriazolium residue and methyl substituents on the cyclam nitrogens (Figure S16). This may indicate that the conformation of N_{nit} in $[\mathbf{1}]^{2+}$ is not determined by steric constraints imposed by the $[\text{DMC-nit}]^{+}$ ligand. Further insights were obtained from the nature of the singly occupied molecular orbital (SOMO) of $[\mathbf{1}]^{2+}$, which features an antibonding combination of the Ni $d_{x^2-y^2}$ orbital with the N_4 lone pairs of the cyclam ligand (Figure S17). Thus, the d^9 "hole" of the Ni(I) center is located in the N_4 plane of cyclam, which is orthogonal to the plane of the N_{nit} atom. Hence, N_{nit}→Ni σ-donation is negligible, as also indicated in the natural bond orbital (NBO) analysis[12] (Table S4) by the nearly identical occupancy of the N_{nit} sp^2 lone pairs in $[\mathbf{1}]^{2+}$ ($1.92e^-$) and free $[\text{DMC-nit}]^{+}$ ($1.94e^-$). In the absence of σ-donation, repulsive interactions between electrons of the Ni-centered d_{z^2} orbital and of the N_{nit} lone pair possibly explains the pyramidal geometry at N_{nit} in $[\mathbf{1}]^{2+}$. NBO analysis also reveals that the Ni–N_{nit} bond in $[\mathbf{1}]^{2+}$ features a dominating π-interaction, as evidenced by the transfer of $0.29e^-$ from the metal to the π-system of the triazolium ring.

A reasonable agreement between the calculated structures of $[\mathbf{2}\text{-F}]^{2+}$ and $[\mathbf{3}]^{+}$ cations and the EXAFS experiments further validates our theoretical methods (Figure S14, Table S1). For $[\mathbf{2}\text{-F}]^{2+}$ the ground state is calculated to be a triplet, consistent with experiment. Since $[\mathbf{2}\text{-F}]$-$(PF_6)_2$ was generated in CH_3CN, which is a potential ligand, we also calculated the structure of the $[\mathbf{2}\text{-}CH_3CN]^{3+}$ species with a bound CH_3CN instead of a fluoride. While DFT calculations also support a S_T = 1 ground state for $[\mathbf{2}\text{-}CH_3CN]^{3+}$, the calculated geometry shows a set of four shorter Ni–N distances of 2.17 Å and two long Ni–N distances of 2.34 Å, which is not in agreement with the EXAFS studies (Table S1). Notably, oxidation of $[\mathbf{1}]^{2+}$ to $[\mathbf{2}\text{-F}]^{2+}$ or $[\mathbf{2}\text{-}CH_3CN]^{3+}$ involves the loss of an electron from the d_{z^2} orbital, and the additional SOMO in $[\mathbf{2}\text{-F}]^{2+}$ or $[\mathbf{2}\text{-}CH_3CN]^{3+}$ is given by an antibonding combination of the d_{z^2} orbital and N_{nit} lone pair (Figure S18). This explains the increased N_{nit}→Ni σ-donation in $[\mathbf{2}\text{-F}]^{2+}$ and $[\mathbf{2}\text{-}CH_3CN]^{3+}$ with respect to $[\mathbf{1}]^{2+}$, as evident from the NBO analysis (Tables S5 and S6), also reflected in the predicted nearly coplanar geometry at N_{nit} in $[\mathbf{2}\text{-F}]^{2+}$ and $[\mathbf{2}\text{-}CH_3CN]^{3+}$ (Figure S14). Furthermore, in contrast to $[\mathbf{1}]^{2+}$, no significant π-back-donation from Ni occurs in $[\mathbf{2}\text{-F}]^{2+}$ and $[\mathbf{2}\text{-}CH_3CN]^{3+}$.

For the $[\mathbf{3}]^{+}$ cation, the ground state can be best described by a broken-symmetry (BS) solution, where the Ni is in a five-coordinate geometry (Figure S14) and a Ni-based d_{xz} orbital is

dx.doi.org/10.1021/ja4099559 | J. Am. Chem. Soc. 2014, 136, 582–585

coupled antiferromagnetically to a N_{nit}-based ligand radical (Figure S19), thereby resulting in a $S_T = 0$ state. The closed-shell (CS) calculation for $[\mathbf{3}]^+$, however, reveals a four-coordinate geometry (Figure S14), with one of the N atoms of the [DMC-nit]$^+$ macrocycle remaining out of the coordination sphere. Interestingly, the CS state is only 3 kcal/mol higher in energy than the BS state. This implies that $[\mathbf{3}]^+$ may coexist in both four- and five-coordinate states, which may account for the structural disorder observed in the EXAFS experiments. Notably, $[\mathbf{3}]^+$ involves a reduced ligand in both the CS and BS states, in full agreement with the experiment; the population of the π-system of the triazolium ring is calculated to be 0.74e$^-$ and 0.91e$^-$ larger in $[\mathbf{3}]^+$ for the CS and BS states (Tables S7 and S8), respectively, than in the free ligand.

Recently, it has been shown that, for a series of Ni(II) complexes, the presence of a basic pendant amine on the ligand backbone plays an important role in the oxidation of formate to carbon dioxide and a proton.[13] With the availability of [**1**]-$(PF_6)_2$, [**2**-F]-$(PF_6)_2$, and [**3**]-(PF_6), we decided to investigate the role of the Lewis-acidic nitrenium cation in the nickel-mediated formate oxidation reactions. Although the Ni(I) centers in [**1**]-$(PF_6)_2$ and [**3**]-(PF_6) are unable to bind and oxidize formate, the Ni(II) complex [**2**-F]-$(PF_6)_2$ is reduced to **1** (45% yield) in the presence of NBu_4HCO_2*HCO_2H or $(HNEt_3)HCO_2$[13] in CH_3CN at 25 °C (Figure S20); CO_2 is produced in 40% yield. Interestingly, reaction of the corresponding $[(TMC)Ni]^{2+}$ complex that lacks the benzotriazolium backbone does not lead to formate oxidation; instead a stable $[(TMC)Ni(HCO_2)]^+$ adduct is formed, the molecular structure of which, as determined by X-ray crystallography (Figure S21), shows a five-coordinate SQP nickel center with the formate bound at the apical position through oxygen.

In summary, we have synthesized and characterized Ni(I) and Ni(II) complexes of a new *N*-heterocyclic nitrenium ligand, [DMC-nit]$^+$, and established an unprecedented bent binding mode of the nitrenium nitrogen to the Ni(I) center that is apparently caused by the presence of a nonbonding electron pair in the N_{nit} sp^2 hybrid orbital. [DMC-nit]$^+$ is a potential non-innocent ligand and can be reversibly reduced by one electron to a neutral ligand π-radical species, both in the free state and when coordinated to a Ni(I) center. Thus, the nitrenium ligands can be considered as NO^+ surrogates,[2e] not only because they are cationic and non-innocent, but also because they can adopt planar or pyramidal coordination modes, analogous to the linear and bent coordination modes of metal nitrosyls.[1a] Furthermore, we have shown that the electrophilic property of a Ni(II) center containing a bound nitrenium ligand can be utilized successfully in the oxidation of formate, thereby supporting the *N*-heterocyclic nitrenium ligand as a potentially useful and versatile reagent in transition-metal-based catalysis. Further studies of the reactivities of [**1**]-$(PF_6)_2$, [**2**-F]-$(PF_6)_2$, and [**3**]-(PF_6) are currently underway in our laboratory, along with possible extension of the coordination chemistry of [DMC-nit]$^+$ to other first-row transition metals and their application in catalysis.

■ ASSOCIATED CONTENT

Supporting Information

Additional syntheses, characterization, kinetic, crystal and computational data, X-ray diffraction parameters. This material is available free of charge via the Internet at http://pubs.acs.org.

■ AUTHOR INFORMATION

Corresponding Author

kallol.ray@chemie.hu-berlin.de

Notes

The authors declare no competing financial interest.

■ ACKNOWLEDGMENTS

We dedicate this paper to Dr. Eckhard Bill on the occasion of his 60th birthday. We gratefully acknowledge financial support of this work from the Cluster of Excellence "Unifying Concepts in Catalysis" (EXC 314/1), Berlin. XAS data were obtained on NSLS beamline X3B (Brookhaven National Laboratory), with support from NIH Grant P30-EB-009998 and the U.S. Department of Energy. F.H. thanks BIG-NSE for a scholarship. We also thank Corinna Matlachowski for help with GC experiments.

■ REFERENCES

(1) (a) Crabtree, R. H. *The Organomentallic Chemistry of the Transition Metals*, 5th ed.; Wiley-VCH: Weinheim, 2009. (b) Duca, G. *Homogenous Catalysis with Metal Complexes*, 7th ed.; Springer: Berlin, 2012.

(2) (a) Dumrath, A.; Wu, X.-F.; Neumann, H.; Spannenberg, A.; Jackstell, R.; Beller, M. *Angew. Chem., Int. Ed.* **2010**, *49*, 8988. (b) Coles, M. P.; Hitchcock, P. B. *Chem. Commun.* **2007**, 5229. (c) Petuškova, J.; Patil, M.; Holle, S.; Lehmann, C. W.; Thiel, W.; Alcarazo, M. *J. Am. Chem. Soc.* **2011**, *133*, 20758. (d) Day, G. S.; Pan, B.; Kellenberger, D. L.; Foxman, B. M.; Thomas, C. M. *Chem. Commun.* **2011**, *47*, 3634. (e) Praneeth, V. K. K.; Paulat, F.; Berto, T. C.; George, S. D.; Näther, C.; Sulok, C. D.; Lehnert, N. *J. Am. Chem. Soc.* **2008**, *130*, 15288.

(3) (a) Tulchinsky, Y.; Iron, M. A.; Botoshansky, M.; Gandelman, M. *Nat. Chem.* **2011**, *3*, 525. (b) Gudat, D. *Coord. Chem. Rev.* **1997**, *163*, 71. (c) Rosenberg, L. *Coord. Chem. Rev.* **2012**, *256*, 606. (d) Caputo, C. A.; Jennings, M. C.; Tuononen, H. M.; Jones, N. D. *Organometallics* **2009**, *28*, 990. (e) Burck, S.; Daniels, J.; Gans-Eichler, T.; Gudat, D.; Nättinen, K.; Nieger, M. *Z. Anorg. Allg. Chem.* **2005**, *631*, 1403. (f) Price, J. T.; Lui, M.; Jones, N. D.; Ragogna, P. J. *Inorg. Chem.* **2011**, *50*, 12810.

(4) (a) Crudden, C. M.; Allen, D. P. *Coord. Chem. Rev.* **2004**, *248*, 2247. (b) Bourissou, D.; Guerret, O.; Gabbaï, F. P.; Bertrand, G. *Chem. Rev.* **2000**, *100*, 39. (c) Marion, N.; Nolan, S. P. *Acc. Chem. Res.* **2008**, *41*, 1440.

(5) Barefield, E. K. *Coord. Chem. Rev.* **2010**, *254*, 1607.

(6) Bosnich, B.; Poon, C. K; Tobe, M. L. *Inorg. Chem.* **1965**, *4*, 1102.

(7) Addison, A.W. T.; Rao, N.; Reedijk, J.; Rijn, J.; Verschoor, G. C. *J. Chem. Soc., Dalton Trans.* **1984**, 1349. For the second independent molecule in crystals of [**1**]-$(PF_6)_2$ $\angle_{sum}$ = 337°, τ = 0.47, Ni–N_{nit} = 1.986(3) Å, average Ni–N(cyclam) = 2.133(3) Å.

(8) (a) Kieber-Emmons, M. T.; Schenker, R.; Yap, G. P. A.; Brunold, T. C.; Riordan, C. G. *Angew. Chem., Int. Ed.* **2004**, *43*, 6716. (b) Jubran, N.; Ginzburg, G.; Cohen, H.; Koresh, Y.; Meyerstein, D. *Inorg. Chem.* **1985**, *24*, 251. (c) Ram, M. S.; Riordan, C. G.; Ostrander, R.; Rheingold, A. L. *Inorg. Chem.* **1995**, *34*, 5884 .

(9) For [**1**]-$(BPh_4)_2$ (Figure S15), g_x = 2.28, g_y = 2.22, and g_z =2.15.

(10) Pal, P. K.; Chowdhury, S.; Drew, M. G. B.; Datta, D. *New J. Chem.* **2002**, *26*, 367.

(11) Colpas, G. J.; Maroney, M. J.; Bagyinka, C.; Kumar, M.; Willis, W. S.; Suib, S. L.; Baidya, N.; Mascharak, P. K. *Inorg. Chem.* **1991**, *30*, 920.

(12) Reed, A. E.; Curtiss, L. A.; Weinhold, F. *Chem. Rev.* **1988**, *88*, 899.

(13) Galan, B. R.; Schöffel, J.; Linehan, J. C.; Seu, C.; Appel, A. M.; Roberts, J. A. S.; Helm, M. L.; Kilgore, U. J.; Yang, J. Y.; DuBois, D. L.; Kubiak, C. P. *J. Am. Chem. Soc.* **2011**, *133*, 12767.